

Supporting Information

Enhanced NO₂-Sensing Properties of Au-Loaded Porous In₂O₃ Gas Sensors at Low Operating Temperatures

Taro Ueda^{1,*}, Inci Boehme², Takeo Hyodo¹ and Yasuhiro Shimizu¹, Udo Weimar² and Nicolae Barsan²

¹ Graduate School of Engineering, Nagasaki University, 1-14 Bunkyo-machi, Nagasaki 852-8521, Japan

² Institute of Physical and Theoretical Chemistry, Eberhard Karls University of Tuebingen, D-72076 Tübingen, Germany

*Correspondence: taroueda@nagasaki-u.ac.jp (T. U.)

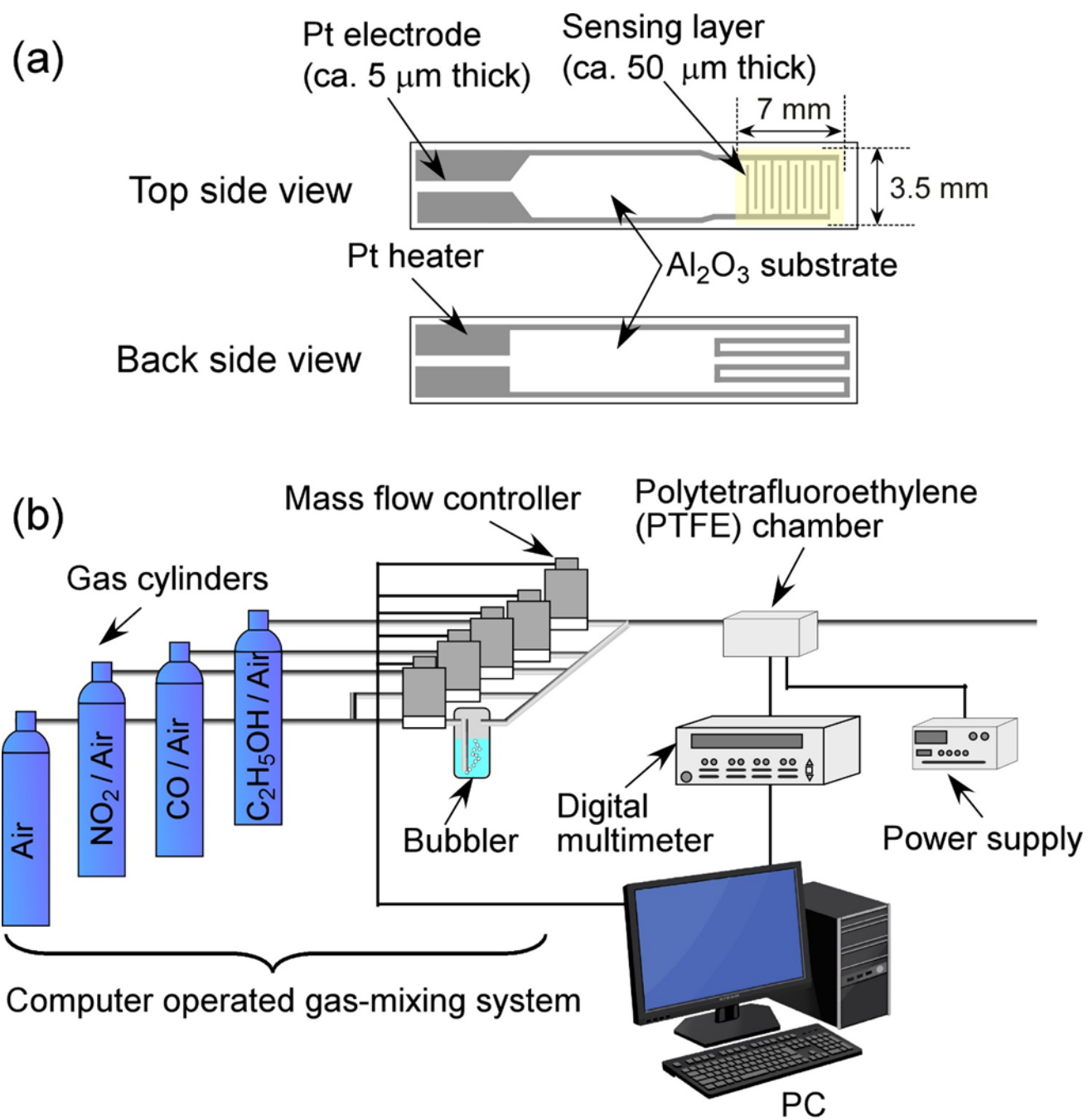


Figure S1. Schematic drawing of (a) sensor element and (b) gas-sensing measurement system.

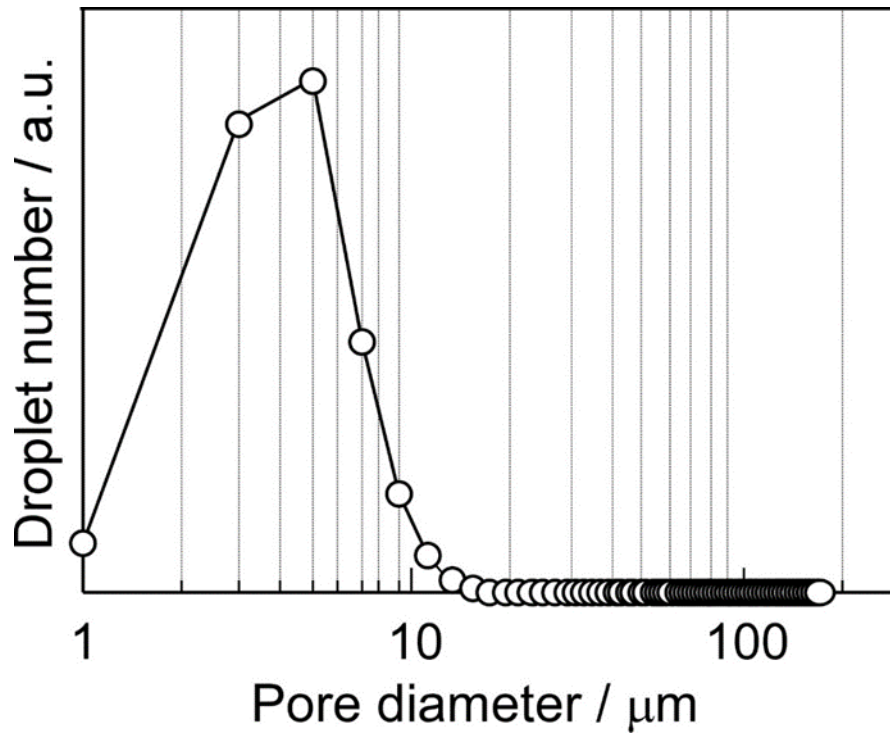


Figure S2. Particle-size distribution of precursor mists containing $\text{In}_2(\text{NO}_3)_3$ and PMMA microspheres, which were prepared by the ultrasonic vibrator.

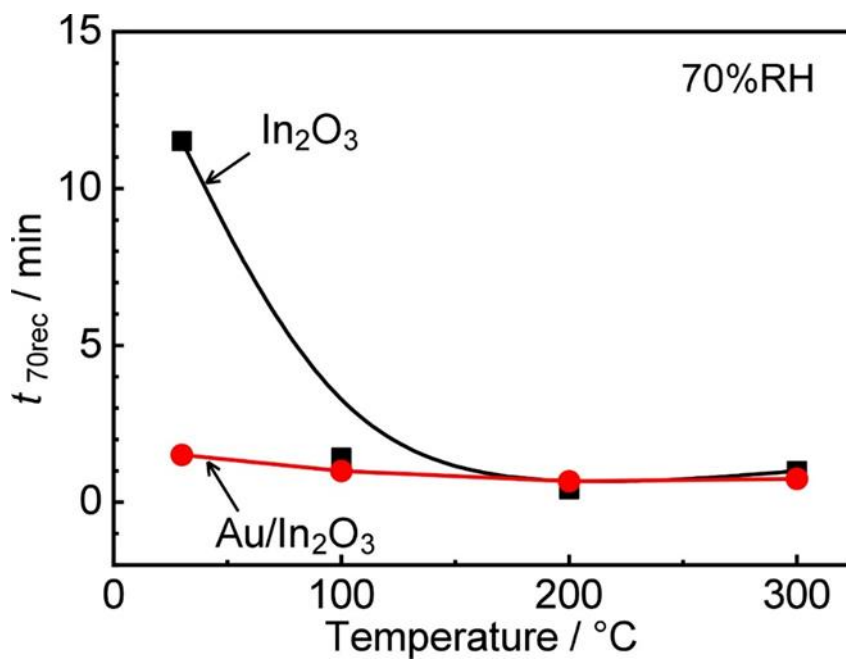
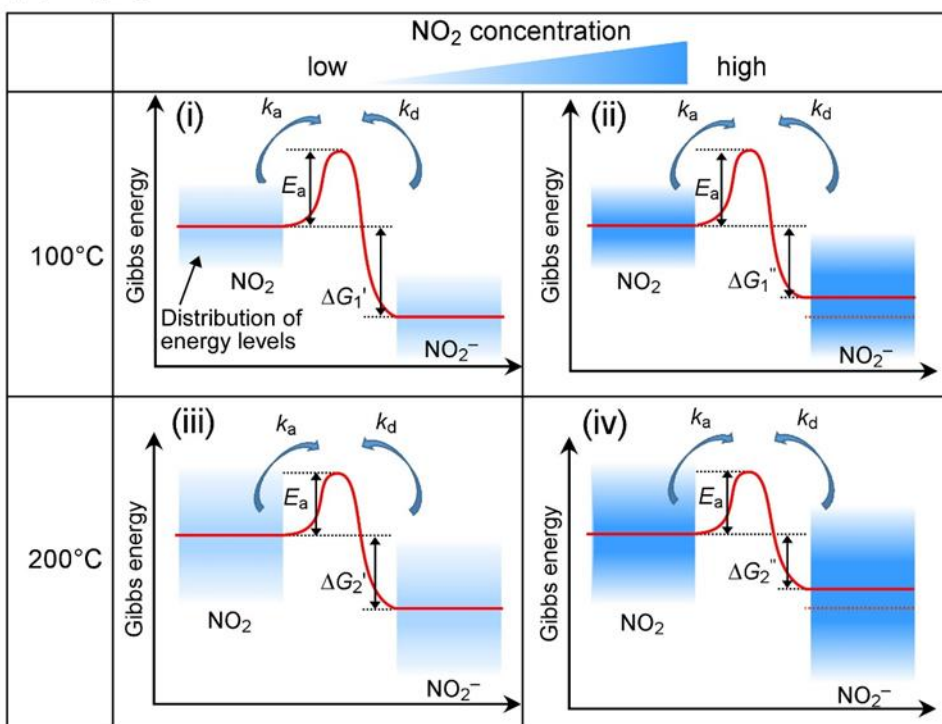
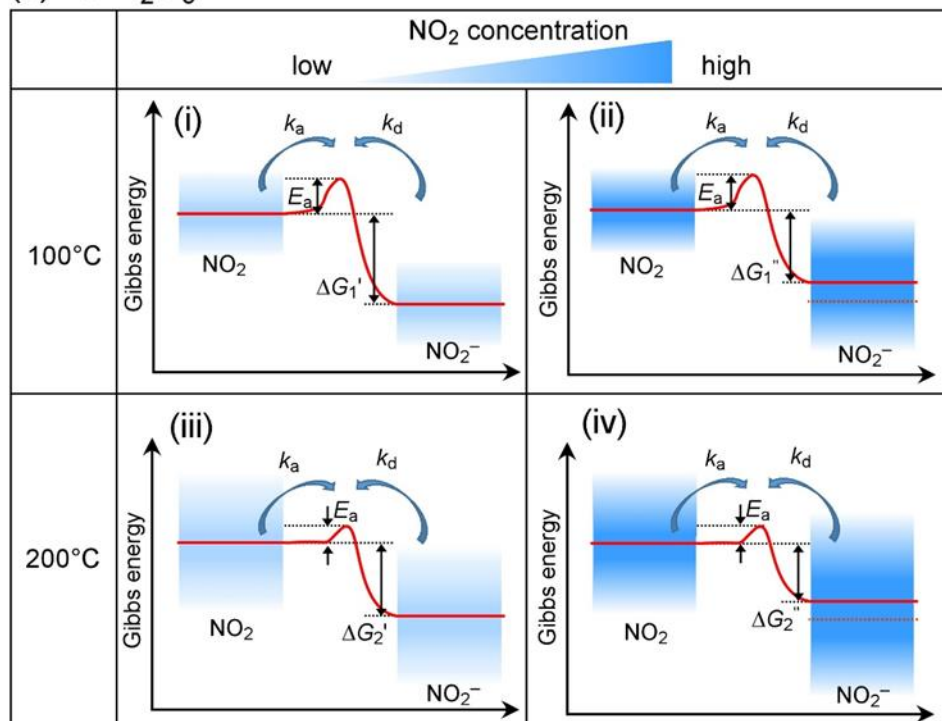


Figure S3. Variations in 70% recovery time ($t_{70\text{rec}}$) of the In_2O_3 and $\text{Au/In}_2\text{O}_3$ sensors in wet air (70%RH at 25°C) with operating temperature.

(a) In_2O_3

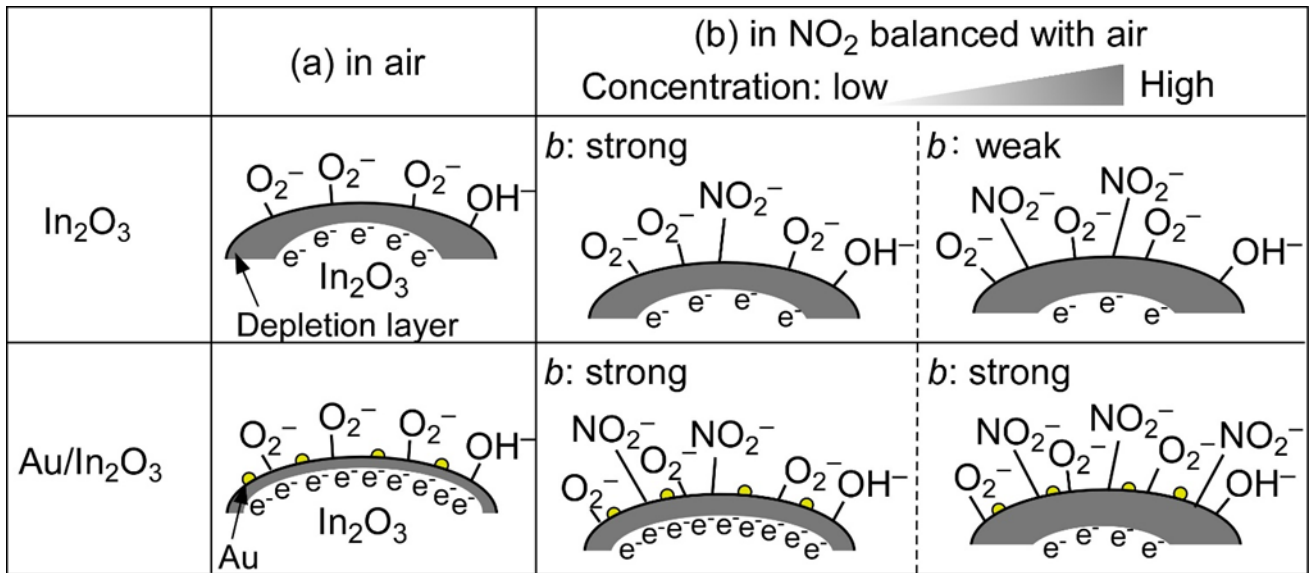


(b) $\text{Au}/\text{In}_2\text{O}_3$



k_a : kinetic constant of adsorption, k_d : kinetic constant of desorption
 E_a : activation energy, ΔG : adsorption Gibbs energy

Figure S4. Schematic illustrations of the Gibbs energy diagram for the chemical adsorption of NO_2 over (a) In_2O_3 surface and (b) $\text{Au}/\text{In}_2\text{O}_3$ surface.



b: adsorption intensity of NO₂ on In₂O₃ surface

Figure S5. Schematic views of gas-adsorption properties of In₂O₃ and Au/In₂O₃ surfaces in wet air and NO₂ balanced with wet air at 100°C.